Reassembly of Flagellar B($\alpha\beta$) Tubulin into Singlet Microtubules: Consequences for Cytoplasmic Microtubule Structure and Assembly

R. W. LINCK and G. L. LANGEVIN
Department of Anatomy, Harvard Medical School, Boston, Massachusetts 02115

ABSTRACT B($\alpha\beta$) tubulin was obtained from a homogeneous class of microtubules, the incomplete B subfiber of sea urchin sperm flagellar doublet microtubules, by thermal fractionation. The thermally derived soluble B tubulin fraction (100,000 *g*-h) repolymerizes in vitro, yielding microtubule-like structures. The microtubule-associated protein (MAP) composition and certain assembly parameters of thermally derived B tubulin are different from those reported for sonication-derived flagellar tubulin and purified vertebrate tubulin. The "microtubules" reassembled from thermally prepared B tubulin are composed of 12–15 protofilaments (73% possess 14 protofilaments). A certain number possess a single "adlumenal component" applied to their inside walls, regardless of the number of protofilaments. Following the first cycle of polymerization, 81% of the B tubulin and essentially 100% of the MAPs remain cold insoluble. Evidence suggests that B tubulin assembles faithfully into a B lattice, creating a j seam between two protofilaments that are laterally bonded in an A-lattice configuration. The significance of these seams is discussed in relation to the mechanism of microtubule assembly, the stability of observed ribbons of protofilaments, and the three-dimensional organization of microtubule-associated components.

Flagellar microtubules represent a class of microtubules uniquely suited for experimental investigation of microtubule structure and assembly, because they can be purified in their native state without need for depolymerization-repolymerization regimens (19, 70). In particular, the B-tubule portion of flagellar doublet microtubules is intriguing, because its native tubulin lattice structure is known (2), and because B tubulin can be selectively purified (67).

In general, the mechanism of flagellar microtubule assembly and, importantly, their stability, have only recently been appreciated. Kuriyama (25) employed sonication to solubilize tubulin from purified sea urchin sperm flagellar doublet microtubules, and demonstrated that the soluble tubulin so obtained would reassemble into singlet microtubules in a manner analogous to the in vitro repolymerization of brain tubulin. Subsequently, Binder and Rosenbaum (6) and Wilson et al. (15, 16, 57) studied more carefully the assembly parameters of soluble flagellar tubulin.

Certain questions were raised by these and other author's work. First, in these studies, 35–40% of the doublet microtubule protein was solubilized by sonication, and the soluble protein was reported to have arisen from both the A and B tubules. Although not stated, it was implied that sonication also solubilized the resistant "ribbon" portion of the A tubule (35). Stephens (67) had previously shown that thermal treatment of purified sea urchin sperm flagellar doublet microtubules selectively solubilized the B subfiber, and that the B subfiber accounted for 35–40% of the doublet microtubule protein. Thus, in the sonication studies (6, 16) it seemed unusual that ~60% of the doublet tubule preparation should remain relatively sonication insoluble, if the A and B tubules were not differentially solubilized. The first question raised here, therefore, concerns the identity of the solubilized doublet tubulin used in the studies mentioned above and how this heterogeneity might have affected the characterization of the in vitro reassembly of the flagellar doublet tubulin.

Second, it was not known whether B tubulin itself could reassemble into complete cylindrical microtubules or could

THE JOURNAL OF CELL BIOLOGY · VOLUME 89 MAY 1981 323–337

only assemble into 10–11-protofilament sheets as it occurs naturally in the B tubule of the doublet microtubule. Stephens (68) had demonstrated that thermally solubilized B tubulin was capable of in vitro polymerization into protofilament sheets, but the solution conditions may not have been optimal for microtubule formation. If it were possible to polymerize purified B tubulin into singlet microtubules, what might be the implications of this achievement for the structure and mechanism of assembly of singlet microtubules in general?

Finally, Binder and Rosenbaum (6) showed that the sonication-soluble "doublet" tubulin reassembled into singlet microtubules which were composed of 14 and 15 protofilaments, instead of 13 protofilaments, as is normally found in A tubules and most cytoplasmic singlet microtubules (29, 74, 77). Were supernumerary protofilament formations due to the possible heterogeneity of A and B tubulin, or were they a result of polymorphism by a homogeneous class of tubulin? Answers here are important to our understanding of the true structure, assembly, and function of microtubules, whether they are of flagellar or nonflagellar origin.

MATERIALS AND METHODS

Purification of Flagellar Doublet Microtubules

Sperm flagellar axonemes were prepared from the sea urchin (*Strongylocentrotus purpuratus*), as previously described (35), by demembranating and homogenizing whole sperm in 1% Triton X-100, 0.15 M KCl, 5 mM $MgSO_4$, 1 mM $CaCl_2$, 0.5 mM EDTA, 10 mM Tris, 1 mM ATP, and 1 mM dithiothreitol (DTT), pH 8.3, at 4°C, followed by differential centrifugation at 2500 *g* for 5.5 min to sediment sperm heads and 13,000 *g* for 7 min to sediment flagellar axonemes. Axonemes were purified and washed by repeated differential spins in 0.15 M KCl, 5 mM $MgSO_4$, 0.5 mM EDTA, 10 mM Tris, 1 mM ATP, 1 mM DTT, pH 8.3, at 4°C. Axoneme pellets were resupsended in 1 mM Tris, 0.1 mM EDTA, 0.5 mM DTT (TED), pH 7.8, 4°C and dialyzed against 100 vol of TED for 18 h. Dialyzed axonemes were diluted with TED and centrifuged at 100,000 *g* for 20 min. The pellets of dialysis-purified doublet tubules were washed a second time by resuspension and recentrifugation in TED.

Fractionation by Thermal Treatment

Pellets of dialysis-purified doublet tubules were resuspended in TED plus 0.1 mM GTP at 0°C, at a protein concentration of 10 mg/ml. To measure the time course of protein solubilization, two samples (S_1 and S_2) of resuspended doublet tubules were first set aside on ice as controls. The remainder in a glass conical tube was brought rapidly to 40°C in a circulating water bath. A timer was set when the temperature reached 39°C, after which the temperature rose to 40°C. Samples were withdrawn after various time intervals, beginning with sample S_3 at t = 0, the time the suspension reached 39°C. Samples were chilled immediately to 0°C in an ice-water bath. Sample S_2 and all the heated samples were then centrifuged at 100,000 *g* for 1 h and the supernates (SS_2, etc.) were collected separately. The protein concentrations of all samples (SS_1, SS_2, ... SS_n) were estimated by the Lowry procedure (43), using bovine serum albumin as the standard of reference. The percent of protein solubilized was calculated relative to the uncentrifuged sample S_1 and corrected for the amount of soluble protein present in the unheated sample SS_2 as follows, and plotted as in Fig. 1:

$$\text{Percent doublet microtubule protein solubilized} = \frac{(SS_n \text{ mg/ml} - SS_2 \text{ mg/ml}) \times 100}{(S_1 \text{ mg/ml} - SS_2 \text{ mg/ml})}.$$

For reassembly studies, a large volume of resuspended doublet tubules (at 10 mg/ml or preferably greater) was brought to 39°C and maintained at a temperature of 39–40°C for 5 min, after which it was rapidly chilled at 0°C in an ice-water bath. Before heating, samples (S_1 and S_2) were taken as described above, for subsequent calculation of the percent of protein solubilized. The chilled sample was then centrifuged at 100,000 *g* for 1 h and the supernate collected for experimental use.

Two factors affect the amount and rate of solubilization of doublet microtubule protein. First, the age of the doublet tubule preparation affects the absolute amount of protein solubilized rapidly. A lower percent of soluble protein is obtained by sonication or thermal fractionation of older preparations. This effect is due partially to the gradual solubilization of doublet tubule protein on standing and is directly attributable to the loss of the more labile B tubule. A preparation of doublet microtubules purified by Tris-EDTA dialysis and stored at 0°–4°C loses ~6% of the 100,000-*g* sedimentable protein/d (data not shown). Care was taken in these experiments to use doublet microtubule preparations immediately after an 18-h Tris-EDTA dialysis. Under such conditions, the amount of protein solubilized rapidly by sonication or thermal fractionation was never >40% and was usually between 32 and 38%.

The second and more technical factor affecting these solubilization curves was the exact detail of the thermal fractionation procedure. The rate of solubilization was critically dependent on the volume of sample and the vessel in which it was heated, and thus on the speed with which the sample reached the temperature of fractionation (39°–40°C). Such conditions did not, however, affect the final extent of solubilization.

Fractionation by Sonication

Pellets of purified doublet tubules were resuspended in 10 mM morpholinoethane sulfonic acid (MES), 0.5 mM $MgCl_2$, 1 mM EGTA, 1 mM DTT, 1 mM GTP, pH 6.7, at 0°C, at a protein concentration of 10 mg/ml. The time-course of solubilization was determined in a manner analogous to that described above for thermal fractionation, except that the suspension was sonicated with a factory calibrated Braunsonic sonicator (Model 1510; B. Braun and Melsungen AG, Melsungen, W. Germany) with a 4 mm diameter microprobe tip. Application of ultrasound consisted of 1-min pulses at 100 W separated by 1 min of cooling; the suspension was continuously maintained in an ice-water bath during sonication.

Polymerization of Tubulin

For preparative reassembly (see Table I), the initial heat-soluble protein was diluted with polymerization buffer concentrate to a final concentration of 10 mM MES, 0.15 M KCl, 10 mM $MgCl_2$, 1 mM EGTA, and 1 mM DTT, pH 6.7, at 0–4°C. This preparation was centrifuged at 100,000 *g* for 30 min, at 3°C, to yield the first cold-soluble (supernate) and first cold-insoluble (pellet) protein fractions. GTP was added at a final concentration of 2 mM to the first cold-soluble fraction; this suspension was then brought to 37°C. Polymerization was allowed to proceed for 30 min, after which the material was centrifuged at 100,000 *g* for 30 min, at 37°C, to yield the first warm-soluble protein fraction and the first warm pellet (one time reassembled microtubules). The first warm pellet was resuspended in two-pellet vol of polymerization buffer minus GTP, as described above, and allowed to incubate on ice for 1 h. This material was centrifuged at 100,000 *g* for 30 min, at 3°C to separate the second cold-soluble and second cold-insoluble protein fractions. To the second cold-soluble fraction was added GTP at a final concentration of 2 mM. This suspension was then incubated at 37°C for 30 min, after which it was centrifuged for 1 h at 100,000 *g*, at 35°C, to yield the second warm pellet (twice reassembled microtubules) and the second warm-soluble protein fraction. Throughout this procedure samples were taken for analysis by electron microscopy (EM), Lowry protein determination, and SDS gel electrophoresis.

For kinetic analysis, the second cold-soluble protein fraction was first brought to the desired temperature; then GTP was then added at a final concentration of 2 mM to initiate polymerization. Microtubule assembly was measured by turbidity as the rate of change in absorbance at 350 nm, using a Gilford recording spectrophotometer (Gilford Instrument Laboratories Inc., Oberlin, Ohio) equipped with a temperature-controlled cuvette chamber. In none of the reassembly studies were flagellar microtubules or soluble tubulin ever exposed to glycerol.

Electron Microscopy

Materials for thin-section analysis were fixed as pellets in 6% tannic acid, 1% glutaraldehyde, 0.15 M sodium phosphate, pH 6.7, for 12 h. Fixed pellets were washed with sodium phosphate and postfixed in 2% osmium tetroxide in sodium phosphate. Specimens were dehydrated in ethanol and embedded in Epon 812 resin. Thin sections were stained with uranyl acetate and lead citrate and viewed in a JEOL 100S or 100 CX electron microscope. For negative staining, a drop of the specimen was applied to carbon-film grids, washed with the appropriate buffer, and stained with 1% uranyl acetate.

Polyacrylamide Gel Electrophoresis

SDS-polyacrylamide gel electrophoresis (PAGE) was carried out using the discontinuous Tris-glycine-SDS system of Laemmli (26). Slab gels were cast with a 7% acrylamide running gel and a 3% stacking gel. Electrophoresis was carried out at a constant voltage of 100 V until the tracking dye reached the bottom of the gel. Gels were stained with 0.025% Coomassie Brilliant Blue R in 25% isopropanol and 10% acetic acid, and were destained in 10% acetic acid.

Molecular weight determinations were made by SDS gel electrophoresis (65, 79), as modified by Laemmli (26). Protein standards used are as follows (except where noted, all materials from Sigma Chemical Co., St. Louis, Mo.): rabbit skeletal muscle myosin (a gift from Dr. Susan Lowey, Brandeis University), 200,000 daltons (42), rabbit muscle phosphorylase A, 94,000 daltons (75); bovine serum albumin, 68,000 daltons (73); bovine liver catalase, 60,000 daltons (72); bovine liver L-glutamic dehydrogenase, 53,000 daltons (75); rabbit skeletal muscle actin (a gift from Dr. Thomas Pollard, Johns Hopkins Medical School), 45,000 daltons (60); and rabbit muscle α-tropomyosin (a gift from Dr. Carolyn Cohen, Brandeis University), 35,000 daltons (23). The molecular weight of 330,000 daltons was used to reference the dynein 1 A band appearing in axoneme preparations (21).

RESULTS

Solubilization of the B Tubule

Purified preparations of flagellar doublet microtubules were fractionated by two different procedures—sonication and thermal fractionation. The two procedures were compared on the basis of the amount of protein solubilized and the structural-chemical identity of the fractionated components. Preparations of doublet microtubules were either heated to 40°C or sonicated at 100 W at 0° for various lengths of time. After heating or sonication aliquots were taken and chilled on ice for further use.

To determine the amount of protein solubilized, the aliquots were centrifuged at 100,000 *g* for 45 min; the amount of protein in the supernates was estimated by the Lowry procedure (43) and expressed as the corrected percent (see Materials and Methods, Fractionation by Thermal Treatment), as shown in Fig. 1. Although the absolute rates of solubilization are different, the result of sonication and thermal fractionation are similar: the rates of solubilization are biphasic, and ~32–36% of the protein is solubilized rapidly. After that, the rate of solubilization is much less. If straight lines are drawn through the fast and slow rates, they intersect at a point that is a convenient measure of the percent of protein solubilized rapidly.

Figs. 2–5 show the ultrastructure of doublet microtubules before and after fractionation. Before fractionation, the material is composed of isolated doublet microtubules; in the fresh preparations used here, singlet microtubules account for <10% of the population (estimated from cross sections). In cross sections of tannic acid–fixed material (Fig. 2 *d–g*), the A tubule can be recognized as a complete cylinder of 13 protofilaments with an "adlumenal component" located over protofilament A_{13} which is adjacent to protofilament A_1, which in turn makes contact with the inner B tubule junction (see Fig. 3 and reference 35). Note that the 10-protofilament B tubule spans an arc of five protofilaments of the A tubule, as shown previously (6, 35, 74, 77), not three protofilaments (24). In negative stain (Fig. 4), the A tubule can sometimes be distinguished by certain criteria: first, the lumen of the B tubule is usually more completely filled with stain than that of the A tubule. Second, a bright ribbon of three protofilaments can be seen in profile lying in the coaxial plane of the A and B tubules; this ribbon remains with the A tubule when portions of the B tubule are lost (Fig. 4 *a*). Occasionally, it can be seen extending beyond the termination of the complete A tubule (35, 81). Finally, a striking axial modulation in electron density frequently occurs coincident with the A tubule lumen on the side adjacent to the B tubule junction (Fig. 4 *a* and *b*); the frequency of this modulation is 16 nm. This 16-nm axially repeating structure may correspond either to the "adlumenal component" of the A tubule or to the "11th" subunit of the B tubule (Figs. 2 and 3).

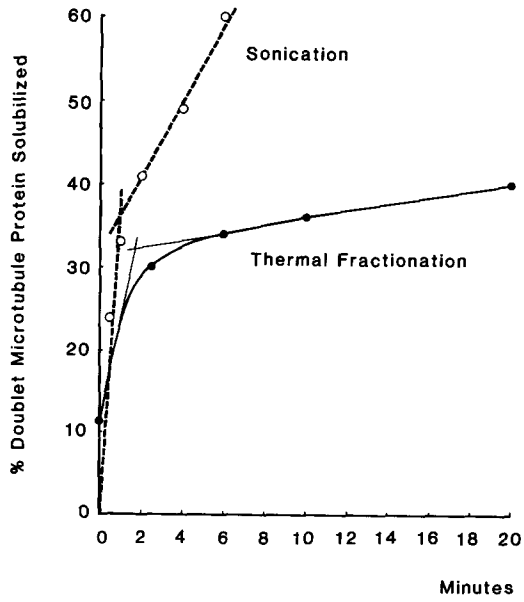

FIGURE 1 Rates of solubilization of doublet microtubule protein after sonication and thermal fractionation. Preparations of doublet microtubules were either sonicated (100 W) or heated (40°C), and samples were taken at various time periods. The percent protein solubilized was calculated and corrected as described in Materials and Methods. The first point on the thermal fractionation curve (11%) originates on the ordinate because the first sample is taken upon reaching 39°C (t = 0 min). Both fractionation procedures yield similar results in that both curves are biphasic, showing a rapid, then a slower, rate of solubilization and in that the intersections of the slopes of the rapid and slow rates (a convenient measure of the protein solubilized during the slow phase) both fall between 32 and 36%.

Results of thermal fractionation of doublet microtubules are shown in Figs. 2 *h–k* and 4 *c–d*. The resultant products are singlet A microtubules, as described originally by Stephens (67). Additional fine-structural details are present: in tannic acid–fixed thin section (Fig. 2 *h–k*), the adlumenal component is frequently retained, applied to the lumenal wall. In negative stain (Fig. 4 *c*), a single row of bright dots with an axial repeat of 16 nm appears superimposed over the lumenal wall. When a portion of the B tubule remains on the A tubule, as in Fig. 4 *d*, the row of periodic structures is again seen superimposed over the same edge of the A tubule to which the B tubule remnant is attached.

Negative-stain images of material that has been sonicated at 100 W for 2 min (Fig. 5) indicate that the products consist of short (50–500 nm) lengths of singlet A microtubules. Effectively, no doublet microtubules are seen after 40% of the doublet tubule protein has been solubilized by sonication. Occasionally, short segments of ribbons of three to four protofilaments are seen individually or emanating from the short lengths of the singlet tubules.

Electrophoretic analysis (Figs. 6 and 10) reveals numerous accessory proteins associated with dialysis-purified doublet microtubules. After fractionation by sonication and thermal treatment, the most predominant proteins remain associated with the A tubule in their original stoichiometric amounts; however, in addition to the α and β tubulin derived principally from the B tubule, numerous minor component proteins are

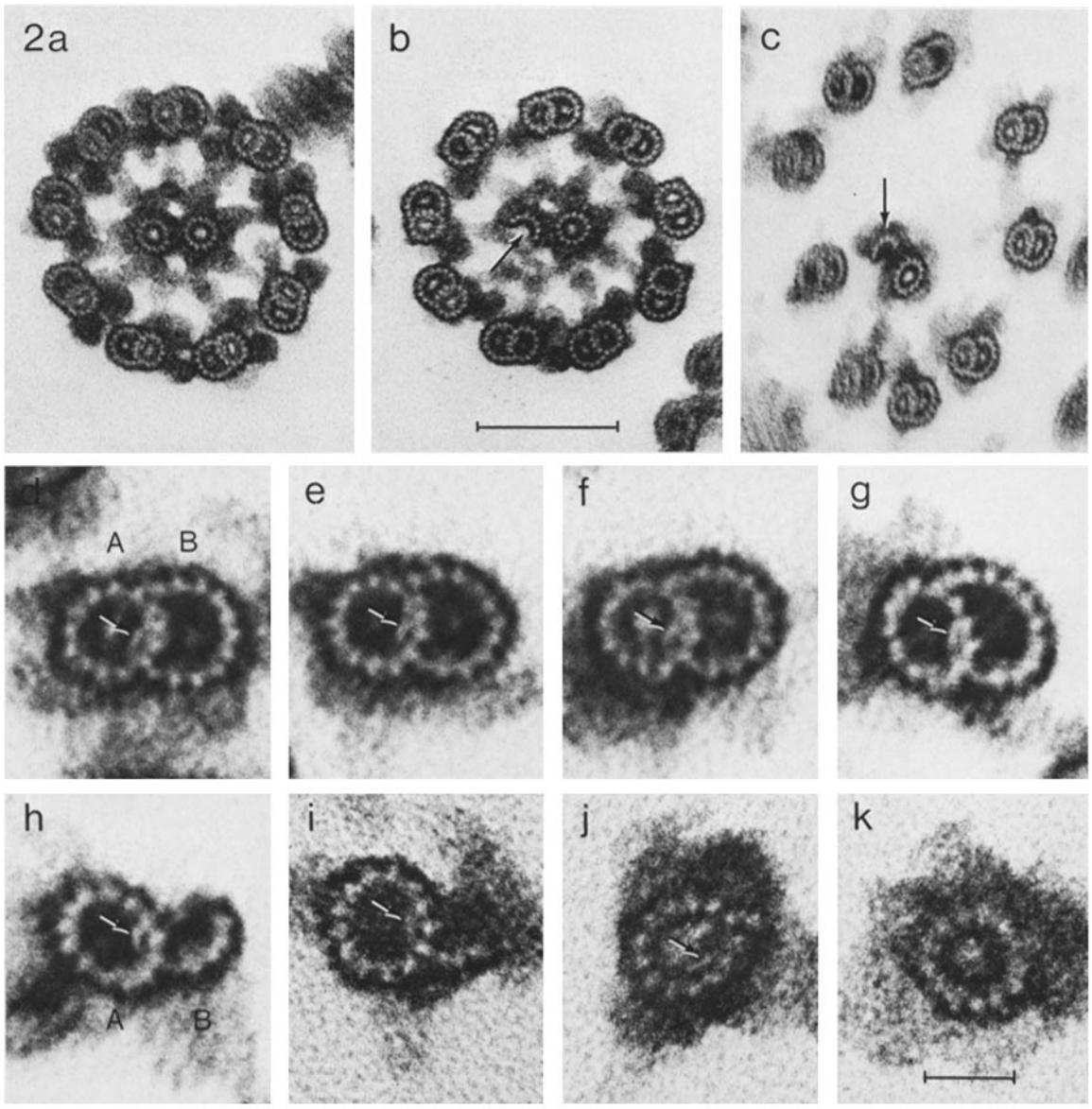

FIGURE 2 Cross sections of tannic acid-glutaraldehyde-fixed flagellar axonemes and flagellar microtubules. *a* and *b*, isolated, demembranated flagellar axonemes. *c*, axoneme after 18-h dialysis against 1 mM Tris, 0.1 mM EDTA, pH 7.8. *d–g*, dialysis-purified doublet microtubules showing substructure of the A tubule, the B tubule, and the "adlumenal component" (arrows). *h–k*, thermally treated doublet microtubules showing the progressive disappearance of the B tubule. After thermal fractionation, A tubules do not orient well enough to provide a meaninful low magnification view; Figs. 2 *i–k* are representative of these thermally prepared A tubules (see also Fig. 4 *c*). Arrows point to adlumenal components. The adlumenal component is positioned adjacent to protofilaments A_1, A_{13}, A_{12}. The structural details of the flagellar microtubules are best seen by comparing these micrographs with Fig. 3; all are arranged in the same orientation for ease of comparison. Occasionally, in isolated axonemes (Fig. 2 *b*), and consistently in dialyzed axonemes (Fig. 2 *c*), one or both of the central-pair microtubules breaks down (arrows), leaving a ribbon of four or more protofilaments. Bars, 0.1 μm for *a–c*, 25 nm for *d–k*.

solubilized (some apparently selectively) by the fractionation procedures. Within the resolution of our electrophoretic analysis, thermal fractionation solubilizes all of those proteins extracted by sonication but also solubilizes others; i.e., polypeptides with molecular weights of ~74, 75, 78, 79, 103, 106, 112, 235, and 285 kdaltons appear to be solubilized substantially more by thermal fractionation (Fig. 6). These polypeptide differences are probably important in explaining the differences in the assembly of crude B tubule prepared by sonication vs. thermal fractionation. It is also important to note that, as shown in Fig. 6, the sarkosyl-resistant nontubulin ribbon proteins are not solubilized to any substantial degree by either fractionation procedure, with the possible exception of a 52-kdalton protein.

The Structure of Reassembled Singlet B Microtubules

The results as described above confirm that thermal fractionation selectively solubilizes the B microtubule of the doublet, as originally shown by Stephens (67), and show that sonication also solubilizes the B tubule during the initial rapid

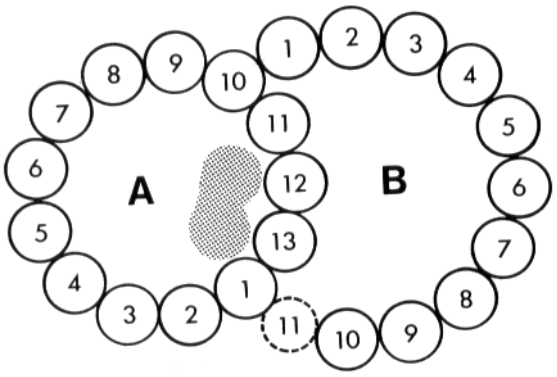

FIGURE 3 Diagram of the cross-sectional view of a sea urchin sperm flagellar doublet microtubule, modified from Linck (35) and Tilney et al. (74). Compare this diagram with Figs. 2, 4, and 8. *A* = A microtubule; *B* = B microtubule; shaded region = adlumenal component. The B tubule is composed of 10 or 11 protofilaments; however, the 11th subunit (broken circle) is frequently missing in cross section, suggesting that it is not a tubulin protofilament but a separate protein involved in the assembly of protofilament B_{10} alongside protofilament A_1. Protofilament 1 of the B tubule is positioned as shown slightly off-center from the A_{10} protofilament. The B tubule thus spans a five protofilament section of the A tubule. The adlumenal component is always situated over protofilaments A_{12}, A_{13}, A_1, as shown, and occasionally appears to be composed of two subunits; a similar but not necessarily identical component also appears in reassembled B singlet microtubules (Fig. 8). The adlumenal component or the 11th subunit of the B tubule may correspond to the 16-nm axially repeating elements seen in negative-stain preparations (Fig. 4). All of the structural features of the doublet microtubule, derived from tannic acid-glutaraldehyde-fixed material, can be seen in previously published micrographs (6, 35, 74).

phase. Soluble B tubulin was prepared by thermal fractionation and subsequent centrifugation, and its ability to reassemble was studied by electron microscopy, gel electrophoresis, and turbidimetric measurements. For reassembly, except as noted, the preparation of B tubulin was brought to final concentrations of 10 mM MES, 0.15 M KCl, 10 mM $MgCl_2$ 1 mM EGTA, 1 mM DTT, 1 mM GTP, pH 6.7, and warmed to 37°C for 30 min.

As illustrated in Figs. 7 and 8, B tubulin under these conditions reassembles mainly into singlet microtubules. In addition, there are other striking features associated with the structure of these reassembled tubules. First, the number of protofilaments forming the walls of the reassembled tubules varies from 12 to 15 and, therefore, may be either odd or even, as seen in tannic-acid thin sections (Fig. 8) or in negative stain (Fig. 7). The frequency distribution of the number of protofilaments per reassembled tubule is shown in Fig. 9; importantly, 73% of the microtubules are composed of 14 protofilaments, whereas all of the remainder are effectively composed of 13 and 15 protofilaments. Second, in preparations of thermally fractionated, reassembled B tubulin, between 5 and 15% of the tubules seen in tannic-acid cross sections possess an additional morphological structure applied to the lumenal wall (Fig. 8). This structure is similar in size to the "adlumenal component" observed in the lumen of the A tubules (Figs. 2 and 3), although positive identification cannot be made at this time. In cross section, it measures 6 × 12 nm and appears in most instances to be composed of two globular subunits ~6 nm in diameter (compare Figs. 2, 3, and 8). What is most striking, however, is that in all of the reassembled microtubules with such structures ($n > 500$), only one adlumenal component is found per cross section of microtubule; furthermore the presence of the adlumenal component is independent of the number of protofilaments per microtubule (Fig. 8). The findings reported above, that microtubules reassemble with 13, 14, and 15 protofilaments and that a single adlumenal component appears in cross sections of the microtubules, regardless of the number of protofilaments, have major consequences on the packing of tubulin subunits in the wall of the microtubules (see Discussion).

Occasionally, structures analogous to doublet microtubules are assembled from B tubulin (Fig. 8 *a* and *g*). Frequently, in such cases the complete singlet microtubule of the doublet analogue possesses a single adlumenal component, and the partial "B-like" tubule assembles onto the outer surface of the singlet tubule across from the adlumenal component, as in the case of native doublet microtubules (Figs. 2 and 3).

Protein Analysis During Cycles of Assembly-Disassembly

The fractionation of doublet tubules by heating and the subsequent reassembly of microtubules through two cycles of assembly were followed quantitatively by protein determinations and qualitatively by SDS-PAGE. These results are summarized in Table I and Fig. 10. These data are from a single experiment, although similar values were obtained when several of the steps were analyzed in repeated experiments. Preparations of thermally fractionated (crude) soluble B tubulin, at 3–3.5 mg/ml in TED, were brought to final concentrations of 10 mM MES, 0.15 M KCl, 10 mM $MgCl_2$, 1 mM EGTA, 1 mM DTT, 2 mM GTP, pH 6.7, incubated on ice for 20 min, and then centrifuged at 100,000 *g* for 30 min; ~17% of the total protein was cold insoluble (Table I). The resultant cold supernate was warmed to 37°C for 30 min; analysis by negative-stain EM of this material indicated the presence of abundant singlet microtubules, as well as some amorphous aggregates. The polymerized material and aggregates were pelleted by centrifugation, resuspended for 1 h in cold polymerization buffer, minus GTP, and centrifuged again. A significant fraction of the protein present in the one-time reassembled microtubules (81%) remained cold insoluble. On addition of 2 mM GTP, and warming to 37°C, the cold-soluble protein polymerized into singlet microtubules with a minimum of nonmicrotubular aggregates (Figs. 7 and 8); 94% of the supernatant protein (tubulin) becomes sedimentable after this second assembly step.

Analysis of the fractionation and reassembly steps by SDS-PAGE is revealing. Relative to the original axonemes (Fig. 10 *a*), flagellar doublet microtubules (10 *b*) are seen to be reduced in the content of the dynein A band (~330 kdaltons) and dynein B band (~285 kdaltons) regions (20, 34) as well as in the content of several lower and two higher molecular weight proteins (3, 21, 61). The flagellar doublet tubule fraction with associated structural components (Fig. 10 *b* and *c*) retains most of the other principle polypeptides, as do the thermal A tubules (Fig. 10 *d*), after purification by heating and centrifugation. Several polypeptides, however, are solubilized by the heat treatment (Figs. 10 *e* and 6 *e*), principally α and β tubulin from the B tubule. On the gel system used, α and β tubulins separate with aberrrant molecular weights of 59 and 56 kdaltons, respectively. In addition, numerous minor component polypeptides are extracted by the heat treatment (dots along lane *e* of

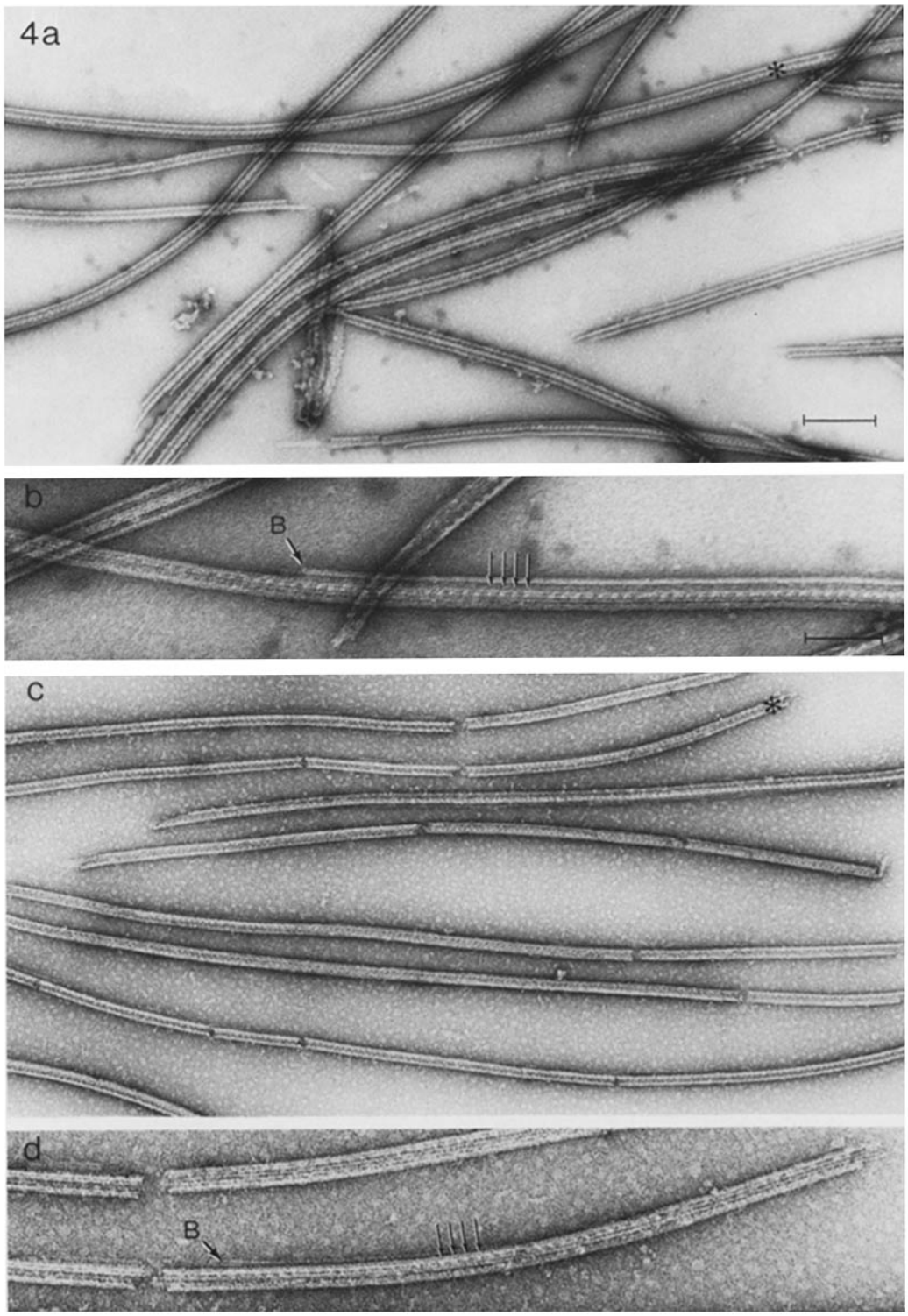

FIGURE 4 Negatively stained preparations of flagellar doublet microtubules (*a* and *b*) and thermally fractionated A microtubules (*c* and *d*). *b* and *d* show high-resolution detail of tubules (asterisks) in *a* and *c*, respectively. In preparations of doublet microtubules, the A tubules can be identified as the more stable tubule after the termination of the B tubule (*B*) and by a row of bright, electron-translucent dots (arrows) superimposed over its lumen on the side adjacent to the B tubule. These dots repeat with an axial periodicity of 16 nm, and they most likely correspond to either the "adlumenal components" or the "11th" subunits of the B tubule seen in cross sections of A tubules (see Figs. 2 and 3). After thermal fractionation (*c* and *d*), the electron-translucent dots (arrows) with an axial repeat of 16 nm can occasionally be seen, again positioned over/in the lumen of the A tubule on the side adjacent to a remnant of the B tubule wall (*B*). Bar in *a*, 200 μm for *a* and *c*; bar in *b*, 100 μm for *b* and *d*.

Fig. 10); some of these appear to be selectively solubilized, including proteins with molecular weights of 72, 73, 76, 77, 84, 95, 103, 235, and 285 kdaltons, in reasonably close agreement with Fig. 6*e*. There appears to be no highly specific cold precipitation of any of these proteins after addition of cold assembly buffer and subsequent centrifugation (Fig. 10*f* and

FIGURE 5 Negatively stained preparation of doublet microtubules after sonication and the resulting solubilization of 36% of the doublet microtubule protein. Note that only short lengths of singlet A microtubules and some ribbon structures of three or more protofilaments (arrows) remain. Compare with Fig. 4c. Bar, 200 μm.

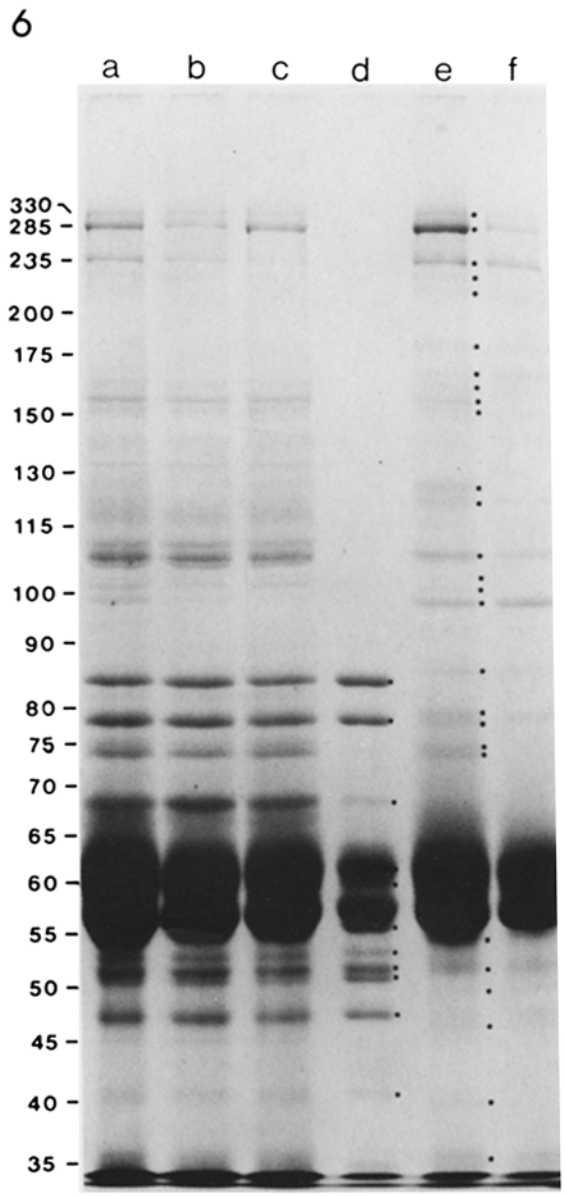

FIGURE 6 SDS-PAGE analysis comparing the effects of thermal fractionation and sonication on the solubilization of doublet microtubule proteins. Lane a, 37.5 μg of doublet microtubules (from 18-h TED dialysis); lane b, 30 μg of thermal A tubules (pellet derived from 37.5 μg of doublet tubules after heating); lane c, 30 μg of sonic A tubules (pellet derived from 37.5 of μg doublet tubules after sonication); lane d, 10 μg of sarkosyl ribbons (pellet derived from 0.75% sarkosyl extraction of 37.5 μg of doublet tubules); lane e, 18.5 μg of thermal solubilized protein (supernate from sample b; two times the amount of protein derived from 37.5 μg of doublet tubules); lane f, 15 μg of sonication solubilized protein (supernate from sample c; two times the amount of protein derived from 37.5 μg of doublet tubules). Numbers on left are a calibrated scale of molecular weights. Dots indicate positions of protein bands visible in lanes *e–f*, not all bands are visible after photographic reproduction. The major proteins solubilized are α and β tubulins with apparent molecular weights (on Laemmli [26] gels) of 61,000 and 57,000 daltons, respectively (actual molecular weight for both is 54,000; see references 7 and 30). Numerous polypeptides are solubilized (some apparently selectively) by thermal fractionation and sonication. Within the resolution of this electrophoretic analysis, thermal fractionation solubilizes all of those proteins extracted by sonication and also solubilizes others.

g), unless the three proteins migrating in the 55- to 60-kdalton regions are not tubulin. Following the first cycle of assembly into singlet microtubules, nearly all of the polypeptides from the previous cold-soluble supernate become sedimentable (designated by dots along lane *h*). Although we have not quantified this analysis, no major fraction of any specific polypeptide appears to remain warm soluble. Surprisingly, in the following step, the cold depolymerization of the one time reassembled tubules, much of the tubulin, and essentially all of the nontubulin proteins remain insoluble in cold assembly buffer (Fig. 10*i*, compared with Fig. 10*h*); the cold-soluble protein consists of essentially pure α and β tubulins (Fig. 10*j*) which represent >95% of the protein as measured by gel densitometry (data not shown). This cold-soluble tubulin fraction reassembles a second time, yielding sedimentable microtubules (Figs. 7, 8, and 10*k*). On underloaded samples of thermally fractionated and reassembled B tubulin the α tubulin region is often seen split into two equally stained bands (Fig. 10*f*, *i*, and *l*, and gels not shown).

Kinetics and Conditions of Assembly

The optimum temperature of polymerization of crude thermal B tubulin (i.e., from step 5, Table I) was measured by spectrophotometric (turbidimetric) assay. The results are shown in Fig. 11. A rapid rise in the rate of assembly takes place above 25°C and reaches an optimum at ~37°C. There is a low but measurable development of turbidity at 20°C, which is probably partially due to nonspecific aggregation of nontubulin

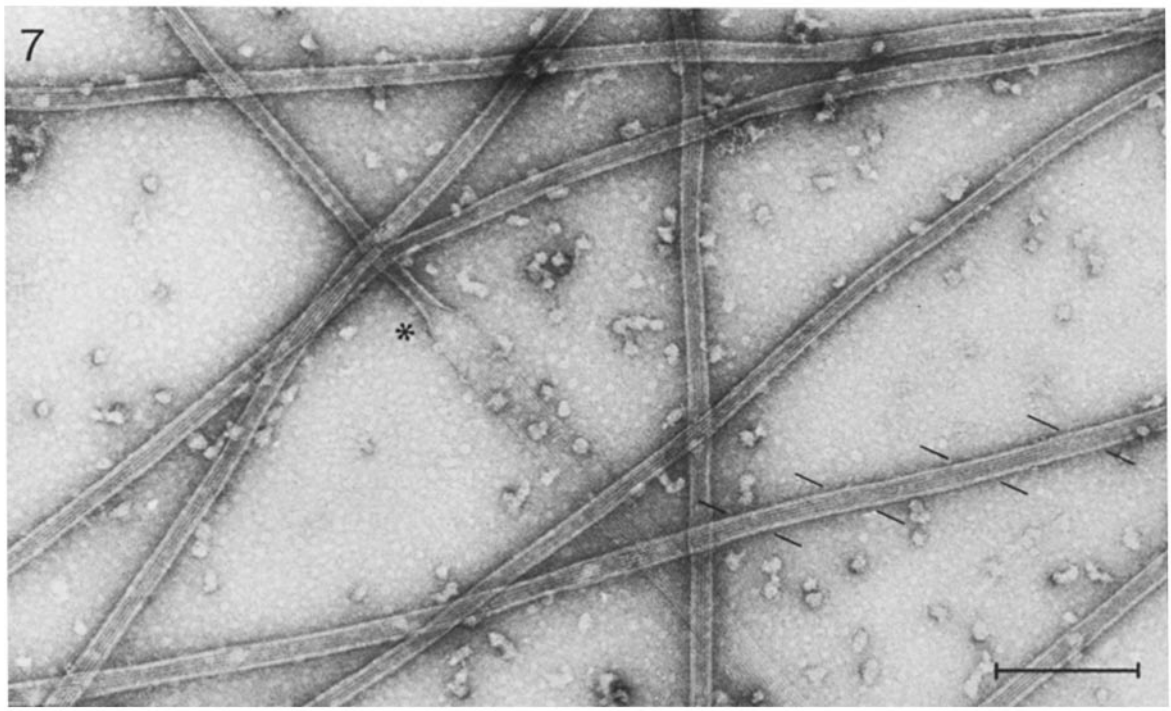

FIGURE 7 Negatively stained preparation of twice-reassembled flagellar B tubulin. A ribbon of 12 protofilaments can be seen closing (at the asterisk) into a microtubule. It is not clear whether this appearance is an artifact of negative stain (e.g., an opening up of a preformed tubule), or whether the closing of a preformed ribbon is an active process in microtubule assembly, possibly mediated by the adlumenal subunit protein at the seam in the microtubule lattice (see Fig. 13). Frequently, a modulation is seen along reassembled B tubulin singlet microtubules (diagonal lines) with an axial periodicity of ~90 nm. Such an appearance has been attributed to the twisting of the microtubule about its axis and, so, the production of a periodic moiré pattern (28). Bar, 100 nm.

protein and/or tubulin, but may also be due to a low level of microtubule assembly. Because a considerable fraction of the microtubule protein reassembled for the first time remains cold insoluble (Table I, step 8, Fig. 10*i*), it has not yet been possible to separate the nonspecific aggregation from events in microtubule assembly that might take place at 20°C.

Microtubule assembly was also measured as a function of protein concentration, using B tubulin which was cycled through one previous reassembly step and which by SDS gel densitometry was determined to be >95% pure. The results are shown in Fig. 12. The data show an extrapolated value of 0.3 mg/ml for the minimum protein concentration required for a change in turbidity and hence significant assembly. Given our estimate of >95% purity, the actual minimum protein concentration may be <0.285 mg/ml. In a separate experiment, a single protein determination of the two times warm-soluble protein (step 10, Table I) yielded a value of 0.17 mg/ml. This minimum value was at least twice as high (0.7 mg/ml) when the initial thermal-soluble B tubulin was used after removal of cold-insoluble aggregates.

Because it had been reported that sonication-solubilized flagellar doublet microtubule protein does not assemble in the absence of added KCl, we assayed the polymerization of thermally solubilized B tubulin for its dependence on salt concentration and obtained a different and important result. Heat-solubilized B tubulin rapidly assembled in the absence of added KCl, i.e., in 10 mM MES, 10 mM $MgCl_2$, 1 mM EGTA, 2 mM GTP, 1 mM DTT, pH 6.7. However, the structures formed are not microtubules but "macrotubules", with diameters of ~45–50 nm and protofilaments that run obliquely to the axis of the tubule at an angle of ~45° (data not shown).

DISCUSSION

Preparation of Reassembly-Competent Flagellar B Tubulin: Sonication vs. Thermal Fractionation

Earlier investigations (6, 15, 16, 25) have established that soluble tubulin can be obtained in a native form by sonication of flagellar doublet microtubules, that this tubulin reassembles in vitro in the presence of only minute quantities of microtubule-associated proteins (MAPs) into singlet microtubules composed of 14 and 15 protofilaments, and that it assembles with kinetics almost indistinguishable from those of purified brain tubulin. These authors indicated that the sonication procedure solubilizes both the A and B tubules and, presumably (though not discussed), the most resistant "ribbons" of three protofilaments of the A tubules (35, 50, 81, 82), even though only 35–40% of the protein was solubilized. These values interested us because B tubulin accounts for only ~35% of the total doublet microtubule protein when the substantial fraction (~25%) of nontubulin proteins are taken into account (35, 67, 68).

We have compared the effects of sonication and thermal fractionation on the same species (*S. purpuratus*) as was used in the studies mentioned above. We find that in early periods both sonication and thermal fractionation solubilize the flagellar B tubule; in later periods, thermal fractionation yields intact singlet A tubules (Fig. 4*c*) and sonication produces very short lengths of A tubules and a small percentage of A tubule–derived ribbons (Fig. 5). The thermal fractionation procedure, because of the greater differential rates of extraction, can yield preparations of B tubulin of high purity. Also, in both procedures, 32–36% of the doublet tubule protein is solubilized rapidly, followed by a more gradual release of protein into

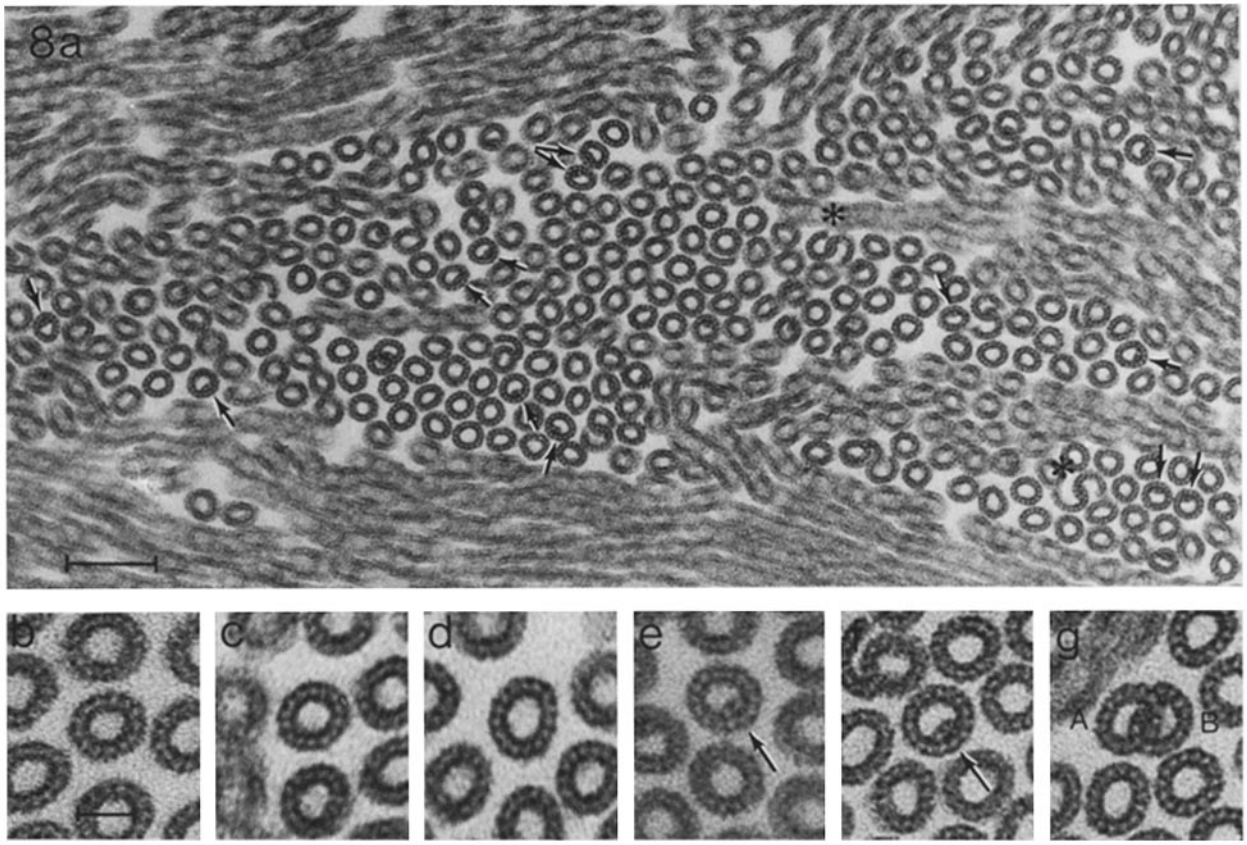

FIGURE 8 Cross sections of twice-repolymerized flagellar B tubulin after fixation with tannic acid, showing microtubule substructure and the adlumenal component. a, low magnification field (from preparation shown in Fig. 10k), showing principally singlet microtubule structures. Each microtubule designated by an arrow possesses one adlumenal component; many other somewhat less clear examples can be seen in this field. S-shaped configurations (asterisks) may represent early stages in the reassembly of doublet microtubule analogues (Fig. 8 *g*). *b–f*, reassembled singlet microtubules composed of 13 protofilaments (b), 14 protofilaments (c), 15 protofilaments (d), 14 protofilaments with adlumenal component attached to inner wall across from arrow (e), and 15 protofilaments with adlumenal component (f). In cross section each adlumenal component appears to be composed of two 6-nm diameter subunits. g, reassembled analogue of a doublet microtubule enlarged from Fig. 8a. The single tubule (A) of 14 protofilaments (with adlumenal component) appears to be the analogue of the A tubule, and the nine-protofilament C-shaped tubule (B), the analogue of the B tubule. Several such doublet-microtubule-like formations have been observed. The appearance of their interlocked walls is an illusion created by the substructure of the adlumenal component. For comparison, see Figs. 2 and 3. Bars, 100 nm for a, 25 nm for *b–g*.

solution (Fig. 1); these results are in agreement with Stephens's (67, 68) kinetics of thermal solubilization of B tubulin. At the point at which 35% of the protein (B tubulin) has been extracted, neither procedure was observed to have solubilized the resistant ribbon fraction (see Fig. 6). It is important to realize, however, that the selective solubilization of the B tubule is not likely to be perfect; because the rates of solubilization are biphasic, we presume a few percent of the A tubule protein is solubilized by the time the B tubule is completely removed. This imperfect selectivity is particularly true in the sonication procedure, where the rate of solubilization of the A tubule presumably approaches that of the B tubule. This effect may partially explain why other investigators have reported observing only doublet tubules following sonication (6, 16), though they showed no micrographs.

The A tubules can be further subfractionated into at least two compartments: first, a soluble fraction (principally tubulin) and second, extraction-resistant ribbons of three to four protofilaments composed of tubulin (35, 50, 81) and several ribbon-specific, nontubulin proteins (Fig. 6*d* and references 35, 36, 39). Thus, any contamination of fractionated B tubulin may result from one or both compartments of the A tubule.

Although both sonication and thermal fractionation appear to be relatively effective in the solubilization of the B tubule and so B tubulin, the two procedures yield soluble fractions whose protein compositions relative to nontubulin proteins differ significantly. With our present level of detection, it appears that the same nontubulin proteins that are extracted by sonication are also removed by thermal fractionation; however, it is clear that several additional proteins are selectively solubilized by the conditions of thermal fractionation. This is probably due largely to the fact that sonication is conducted in the presence of 0.5 mM $MgCl_2$, pH 6.7, at 0°C, whereas thermal fractionation is conducted in the presence of 0.1 mM EDTA, pH 7.8, at 40°C. It should be realized that, in the case of the selectively solubilized nontubulin proteins, they may have originated from either the A tubule, the B tubule, the resistant ribbons, or all three compartments.

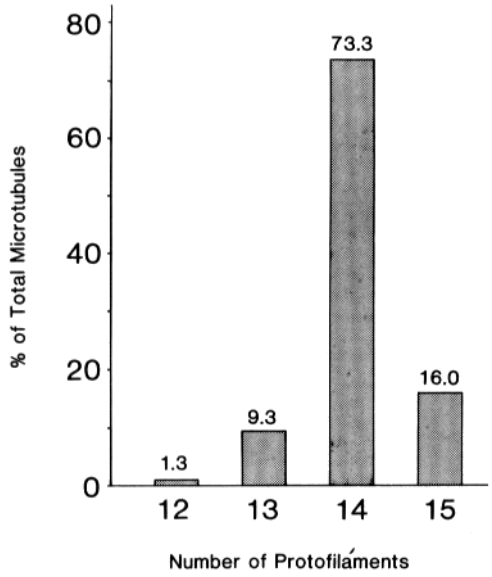

FIGURE 9 Frequency distribution of protofilament numbers per microtubule calculated from thin sections of tannic acid-fixed, twice-reassembled B tubulin microtubules (n = 75), such as those shown in Fig. 8.

TABLE I

Protein Balance during Thermal Fractionation and Reassembly

	Percent				
Fraction or step in reassembly	a	b	c	d	e
1 Doublet microtubules, dialyzed and washed (*c**)	100				
2 Heat-insoluble A microtubules (*d*)	60				
3 Initial heat-soluble protein (*e*)	40	100			
4 First cold-insoluble protein (*f*)	7	17			
5 First cold-soluble protein (*g*)	33	83	100		
6 First warm-soluble protein	4		12		
7 First warm pellet: One time reassembled microtubules (*h*)	29		88	100	
8 Second cold-insoluble protein‡ (*i*)	23			81‡	
9 Second cold-soluble protein (*j*)	6			19	100
10 Second warm-soluble protein	0.5				6
11 Second warm pellet: Two times reassembled microtubules (*k*)	5.5				94

Column *a* gives the total protein balance from the thermal fractionation of doublet microtubules (100%) through two cycles of assembly (warm) and disassembly (cold); the values are relative to the original starting material. Columns *b* through *e* express the percent of soluble and insoluble protein relative to the previous step. Samples *1* through *11* are in the following solutions: Samples *1–3* (1 mM Tris, 0.1 mM EDTA, 1 mM DTT, 0.1 mM GTP, pH 7.8); samples *4–7* (10 mM MES, 1 mM Tris, 0.15 M KCl, 1 mM EGTA, 0.1 mM EDTA, 1 mM DTT, 10 mM $MgCl_2$, 2 mM GTP, pH 6.7); and samples *8–11* (10 mM MES, 0.15 M KCl, 1 mM EGTA, 1 mM DTT, 10 mM $MgCl_2$, 2 mM GTP, pH 6.7).

* Letters in parentheses refer to sample lanes in Fig. 10.

‡ A large fraction of the first-cycle warm-insoluble material (i.e., repolymerized B tubulin and MAPs and nonspecific aggregates) remain cold insoluble in the presence of the reassembly solution.

Biochemical Parameters of Reassembly

There appear to be similarities as well as significant differences in the assembly of protein obtained by the two procedures. The differences may be related to the effects of ultrasound vs. heat on the solubilized protein or, more interestingly, may be related to the presence or absence of different MAP components in the two different soluble B tubulin fractions.

The rate of assembly of thermally prepared B tubulin as a function of temperature (Fig. 11) is similar to that reported for sonication-derived doublet tubulin (15) and for vertebrate brain tubulin (31, 53). The rate of polymerization increases above 20°C and reaches an optimum at 37°C. The rate of polymerization at <25°C is reported to be near baseline after subtracting cold- or podophylotoxin-insoluble material (15).

The efficiency of thermally prepared flagellar B tubulin in repolymerizing is extremely high. After an initial repolymerization and cold-solubilization of tubulin, a value of 0.3 mg/ml was obtained as the critical (i.e., minimal) protein concentration required for a second reassembly (Fig. 12). Given the ~95% purity, the critical tubulin concentration is therefore 0.285 mg/ml, although a single value of 0.17 mg/ml was once obtained. These data are somewhat lower than those reported for sonication-derived proteins (0.55 mg/ml, reference 15; 0.72 mg/ml, reference 6), but the latter values were obtained from the first cycle of repolymerization. Our values for the critical tubulin concentration are also somewhat lower than that reported for purified, MAP-free 6S brain tubulin under rather similar ionic conditions (i.e., 0.5 mg/ml; see reference 31), and resemble more that of brain tubulin during reassembly in the presence of high molecular weight MAPs (~0.2 mg/ml; see references 17, 32, 52, 54, and 64).

Depending on the method of isolation of B tubulin, repolymerization is strikingly affected by the concentration of KCl in the assembly buffer. In sonication-derived tubulin, no assembly was found to occur in the absence of added KCl (6, 15). On the other hand, we find that thermally prepared B tubulin rapidly assembles in the absence of KCl but, instead of forming typical microtubules, it polymerizes to form "macrotubules," 40–50 nm in diameter, whose protofilaments run obliquely to the tubule axis (data not shown). These macrotubules resemble similar structures that have been shown to form in vitro from preparations of brain microtubule protein (14, 27).

A quantitative and qualitative analysis of the yield of protein in the soluble vs. insoluble phases during two cycles of assembly is revealing (Table I). The starting material for the first assembly consists of the protein that is solubilized by thermal fractionation (Table I, step 3) and remains cold soluble after addition of assembly salts (step 5). Of the protein in this fraction, 88% becomes pelletable after warming to 37°C for 30 min (step 7), and of this sedimentable fraction, 81% remains cold insoluble. This cold-insoluble protein is predominantly tubulin, but contains quantitatively almost all of the thermally extracted MAPs (Fig. 10*i*). Two explanations can be given for such a high percentage of tubulin and MAPs remaining insoluble after the first reassembly: first, a large fraction of the tubulin and nontubulin proteins may have been denatured by the thermal fractionation procedure (6 min at 40°C in 1 mM Tris, 0.1 mM EDTA, 0.1 mM GTP, 1 mM DTT, pH 8) and become insoluble at 37°C, but not at 0°C, under the conditions of assembly (principally 10 mM MES, 0.15 M KCl, 10 mM $MgCl_2$, pH 6.7). Although amorphous aggregates are seen in negative stain and thin section after the first warm-induced repolymerization, this material can account for only a small

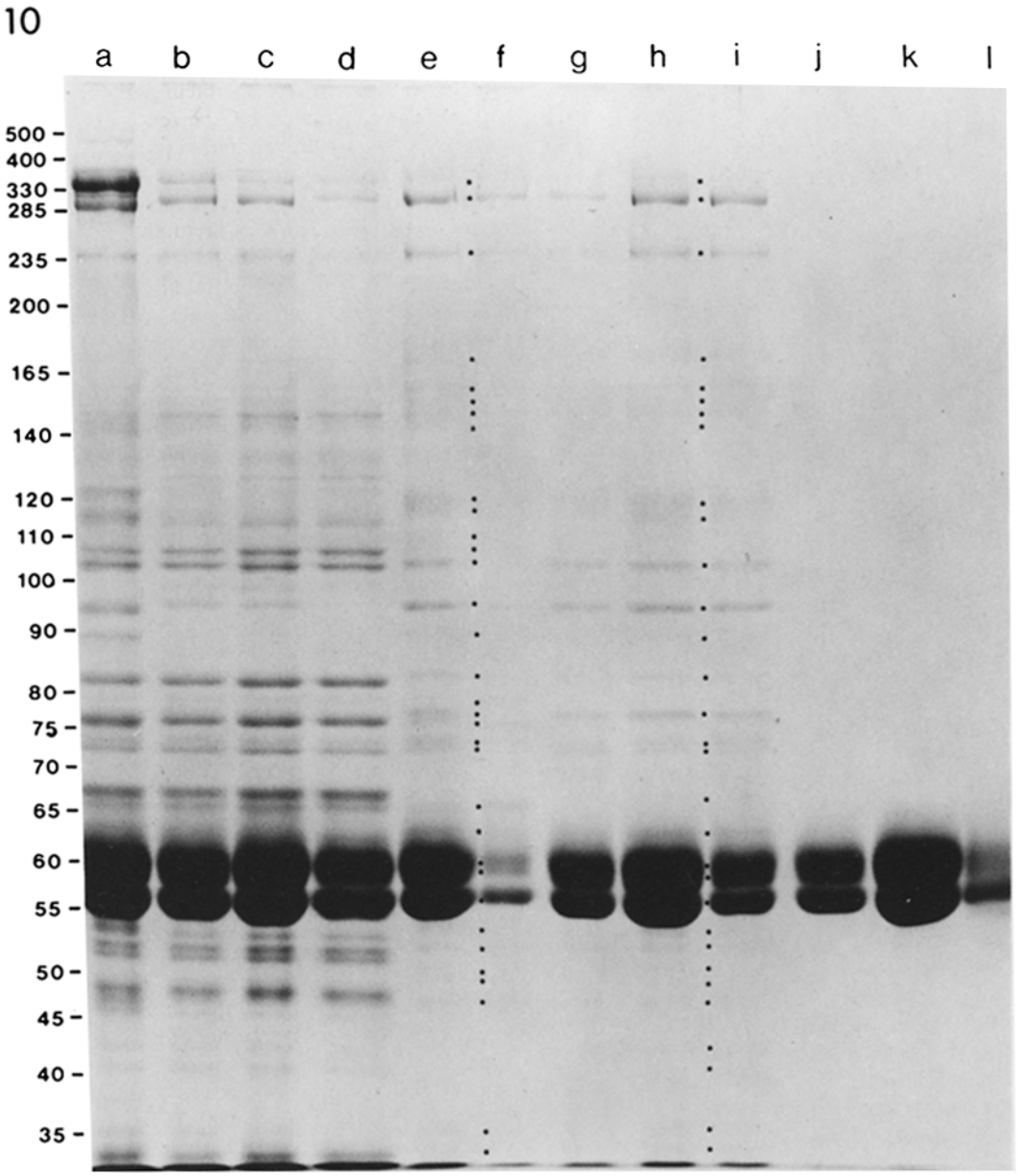

FIGURE 10 SDS-PAGE analysis of axoneme and doublet microtubule fractionation and subsequent steps in the repolymerization of B tubulin. Compare with Table I. Lane a, axonemes (20 μg); b, doublet microtubules (14 μg, from 20 μg of axonemes); c, doublet microtubules (17.5 μg); d, heat-insoluble A microtubules (10.5 μg, from 17.5 μg of doublet tubules); e, initial heat-soluble protein (14 μg, two times the amount from 17.5 μg of doublet tubules); f, first cold-insoluble protein (2.4 μg, from 14 μg of heat-soluble protein); g, first cold-soluble protein (11.6 μg, from 14 μg of heat-soluble protein); h, first warm pellet—one time reassembled microtubules (10 μg, from 14 μg of heat-soluble protein); i, second cold-insoluble protein (4.1 μg, half the amount from 10 μg of one time tubules); j, second cold-soluble protein (3.4 μg, two times the amount from 10 μg of one time tubules); k, second warm pellet—two times reassembled tubules (20 μg); l, same as k (2 μg). The numbers on the left indicate calibrated molecular weights in daltons $\times 10^{-3}$ (k). In e, proteins solubilized by thermal fractionation (designated by dots) are indistinguishable from the equivalent fraction (Fig. 6e) of a different experiment; nearly all of the proteins selectively solubilized by thermal fractionation (lane e) become quantitatively sedimentable during the first reassembly (lane h) and remain cold insoluble (lane i). Note: the α tubulin region (mol $wt_{apparent}$ = 58–60 kdaltons) on underloaded gels frequently splits into two bands (lanes f and l). Not all original faint bands show in the photographic reproduction.

fraction of the sedimentable protein, given the extraordinarily high density of microtubule structures observed by thin-section and negative-stain EM (data not shown). A second and reasonable possibility is that the presence of any one of several MAPs could confer a cold stability to the repolymerized B tubulin (see discussion below), as suggested by Farrel et al. (15, 16) and Webb and Wilson (78). Although our electron microscope examinations have not revealed structurally intact, cold-stable, reassembled microtubules, we do observe abundant filamentous material. The possibility that cold-stable ribbons of protofilaments are formed is considered later in this discussion.

In addition to the possibility of conferring cold stability on microtubules, or portions thereof, one or more of the MAPs may be required for initiation and/or elongation, as originally

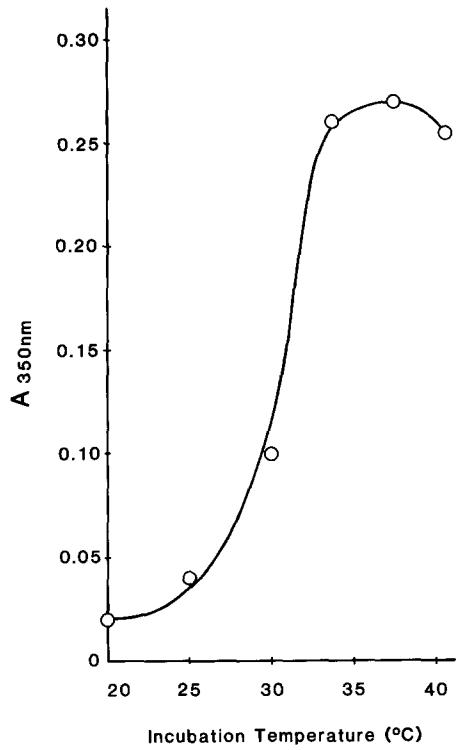

FIGURE 11 Polymerization of B tubulin as a function of temperature. Initial heat-solubilized B tubulin was prepared, adjusted to a final concentration of 10 mM MES, 10 mM $MgCl_2$, 0.15 M KCl, 1 mM EGTA, 1 mM DTT, pH 6.7, and centrifuged. The cold-soluble supernate (fraction 5, Table I) was brought to the desired temperature and adjusted to 2 mM in GTP; immediately, the increase in optical density at 350 nm (A_{350nm}) was recorded for 30 min. The data are plotted as the value of A_{350nm} after a 5-min incubation period.

shown for the 55- to 68-kdalton "tau" protein(s) (9, 10, 24, 56, 64, 80, 83) and the ~270 kdalton, high molecular weight MAPs (12, 51, 64, 66). At present, the crude thermally solubilized B tubulin fraction is too heterogeneous for us to sort out the assembly-promoting contributions of the various portein species; however, the results of the second cycle of reassembly are informative. The preparation of two times reassembled microtubules (see Fig. 10*k*) is >95% pure tubulin, as determined by quantitative SDS-PAGE: three protein bands are occasionally seen (more frequently the upper two bands fuse), designated α_1, α_2, and β tubulins, which separate in a ratio of ~1:1:2, in agreement with the findings of Bibring et al. (5) and Stephens (69). The value of 95% purity of the B tubulin is probably an underestimate, because all minor deviations from baseline are integrated as nontubulin protein. At present, no single protein species besides tubulin is evident in these two times microtubule preparations. Yet, the efficiency of the polymerization reaction is extremely high (critical protein concentration = 0.17–0.285 mg/ml). Thus, we are left with two possibilities: either flagellar B tubulin can assemble in the absence of MAPs and glycerol, at a critical concentration that is one-half that previously reported for MAP-free vertebrate brain tubulin under similar conditions(31), or a potent nucleating protein exists as a contaminant which has so far gone undetected. Such a protein might be active in minute concentrations or might migrate closely with one of the tubulins and be obscured on moderately loaded SDS gels. The possibility that such a potent nucleating protein exists is raised by our ultrastructural analysis (Fig. 8), which reveals the presence of a distinct structural component bound to the inside walls of a certain percentage of the two times reassembled microtubules.

The Structure of Synthetic B Tubulin Singlet Microtubules

Given that the A and B tubules have been shown to possess different dimer lattices—the A and B lattices, respectively (2)—an immediate question raised by this investigation is whether B tubulin polymerize with its own native B lattice into singlet microtubules, or it polymerizes aberrantly with an A lattice. If fidelity of the microtubule structure is not maintained during reassembly, then the relevance and interpretation of many in vitro results must be questioned (see reference 58). On the other hand, if B tubulin does assemble in vitro in the form of a B lattice, then the singlet tubules so formed are helically asymmetric, as is apparent from the geometry of the B lattice (1, 2, 28, 48, 49); i.e., microtubules composed of the B lattice possess a seam between two protofilaments which are bonded in an A lattice-like manner (see Fig. 13).

Although we have not directly determined the lattice structure of the synthetic B tubulin singlet microtubules, evidence supports our belief that fidelity of the lattice is maintained during assembly, i.e., that B tubulin assembles with its native B lattice (Fig. 13). The evidence is as follows:

(*a*) Brain tubulin has been shown to repolymerize into "microtubules" composed primarily of 14 protofilaments in a B-lattice configuration (49; also references 11, 45, and 46). Although the actual structure of native brain microtubules remains unknown, it is reasonable to suppose that if brain tubulin assembles in vitro into a B lattice, then so should flagellar B tubulin, which naturally possesses that lattice.

(*b*) A symmetrical arrangement of dimers, as in the A lattice, is incompatible with "microtubules" composed of even number

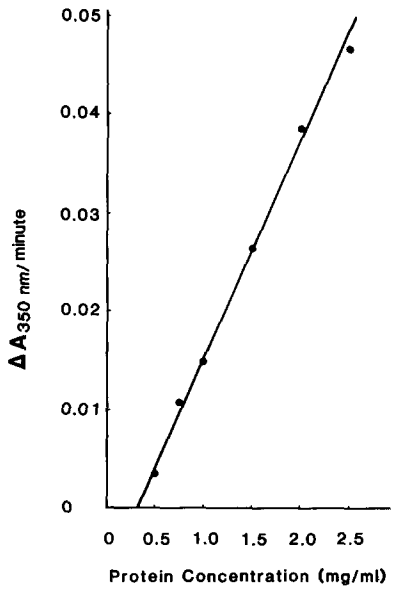

FIGURE 12 Rate of polymerization of B tubulin as a function of the protein concentration. Thermally fractionated B tubulin was assembled once as described in Materials and Methods. The cold-soluble protein from this first assembly was then assayed for its rate of assembly (ΔA_{350nm}/min) at different protein concentrations. The data points fall on a straight line extrapolating to a minimum protein concentration of 0.3 mg/ml. The protein assayed was >95% pure $B_{\alpha\beta}$ tubulin, as judged by densitometry of SDS gels (see Fig. 10k).

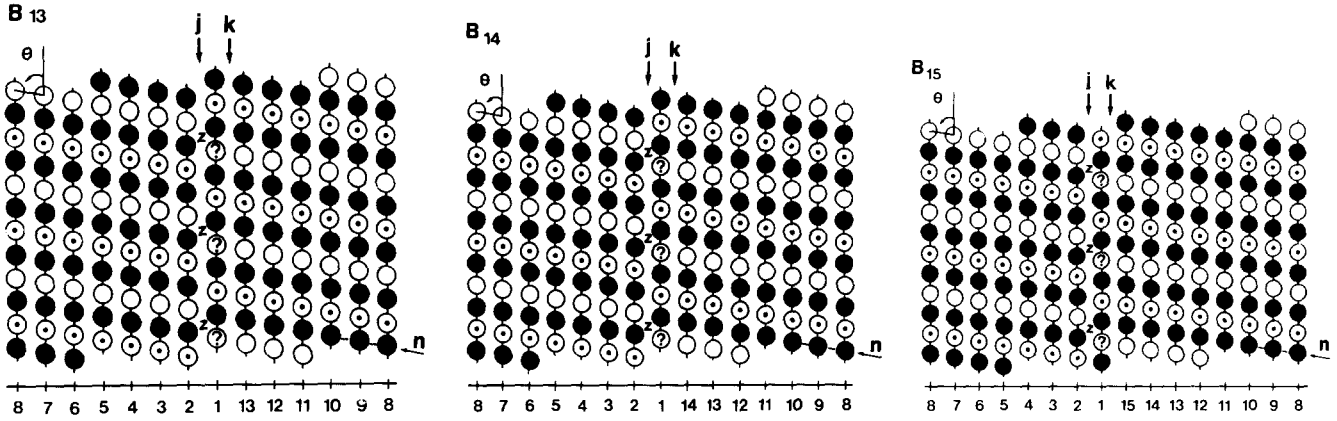

FIGURE 13 The models describe the simplest of several possible lattices of purified B tubulin polymerized in vitro into "microtubules" of 13, 14, and 15 protofilaments. The details are similar to those of model B_{13} in Fig. 13 of the accompanying paper (40): the longitudinal (numbered) protofilaments are composed of α (open circles) and β tubulin (filled circles), thought to form $\alpha\beta$ heterodimers (2, 44). All models possess a left-handed, three-start helical family (*n* arrows) which, with the protofilaments, defines the lattice of monomers and a ~4-nm axial × 5-nm equatorial unit cell (2, 13, 38, 49). θ is the smaller bond angle of the tubulin monomer unit cell. Open circles with dots designate a unique population of α_2 tubulin subunits whose existence, particularly in the B subfiber, is supported by this and other reports (5, 69), although the heterogeneity of tubulins in microtubules appears to be even more complicated (4, 33, 41, 69, 71). For simplicity, we illustrate only the different α_1 (open circles) and α_2 subunits (circles designated by . or ?). For reasons given in the Discussion, we believe that purified B tubulin polymerizes in vitro into its native B lattice configuration, as defined by Amos and Klug (2), with the additional details described above. It has been shown that brain tubulin also assembles in vitro into microtubules with a B lattice (49). Such an arrangement of dimers requires that there be a helical dislocation in the form of a seam between two of the protofilaments bonded in a A lattice-like manner (1, 28, 49); this dislocation is designated here as a j seam (*j* arrow). In the in vitro polymerization of these and brain microtubules, two mechanisms of assembly can be envisaged: first, bonding and elongation of protofilaments 1 and 2 (formation of the j seam) may precede that of the remaining protofilaments. Second, formation of a continuous B lattice may precede the final formation of the j seam. Thus, depending on where α_2 tubulin assembles in protofilament 1 (at . or ?), a second, unique k seam may be formed. These models automatically generate a series of stereospecific sites (e.g., z sites) that repeat at 16 nm along the j seams. The significance of these models to native microtubules is discussed in the text.

of protofilaments (see also references 1, 48, and 49); thus, with the formation of the A lattice, a different mechanism of assembly would be required for "microtubules" formed from even vs. odd numbers of protofilaments. It might thus be expected that "microtubules" containing even numbers of protofilaments would be more thermodynamically favored than those containing odd numbers, or vice versa. Yet the work of Pierson et al. (58, 59) argues against such a conjecture, because it was shown that protofilament distribution patterns of reassembled brain tubulin vary from 9 to 17 in a unimodal fashion and depend on solvent and temperature conditions but show no bimodal distribution of odd vs. even protofilament numbers.

(*c*) The B_{13}, and the B_{14} and B_{15} structures in Fig. 13 (and, in principle, all such B_n structures) are structurally quasiequivalent. According to the theory of Caspar and Klug (8), they are identical in every respect except for slight changes in the bond angle θ on the order of +0.7° per additional protofilament (θ-79.5° for B_{13}). Importantly, the j seams remain equivalent, as do the k seams and z sites. The mechanism of assembly for all B_n models is therefore also quasiequivalent. An energetically more favorable bond angle of $\theta = 80.3°$ is sufficient to explain the essentially Gaussian distribution of the number of protofilaments observed with a single mode of 14 (Fig. 9).

(*d*) Finally, the j and/or k seams can account for the formation or attachment of a single "adlumenal component," regardless of the number of protofilaments (Fig. 8). We do not know the nature of the adlumenal component; it could be a unique tubulin or a nontubulin MAP, or it might arise from a unique arrangement of identical tubulins. Regardless of its origin, the appearance of this component in reassembled microtubules again indicates that the tubulin lattice is helically discontinuous (asymmetric).

The Significance of "Seams" in the Structure and Assembly of Microtubules

In the accompanying paper (40), we have presented evidence that the native central C_2 microtubule of squid sperm flagella is asymmetric and have proposed two models for its subunit lattice, both of which possess seams between certain protofilaments. By independent evidence, we arrive at similar conclusions in this paper and suggest that the B lattice models (Fig. 13) best explain the structure of singlet microtubules synthesized in vitro from B tubulin. We offer these models not as a final solution to the structure of native microtubules, because there may be some aspects that are incomplete or incorrect, but as testable models that illustrate certain fundamental features of microtubules that have not previously been appreciated. Several points deserve comment; these points are as relevant to in vitro polymerized brain and B tubulin singlet microtubules as they are to native microtubules, all of which may possess similar or different types of seams:

(*a*) First, the seams present in these models are potentially important in the assembly of microtubules. In the example of the microtubule diagrammed in Fig. 13, two mechanisms of assembly can be envisaged. In the first case, the *j* seams form first, i.e., the bonding and elongation of protofilaments 1 and 2 precede that of the remaining protofilaments. In the second case, the *j* seams form last, i.e., the formation of a length of a 13 protofilament sheet precedes the final closure into a cylinder

by the subsequent formation of the *j* seam. Due to the presence of *j* seams, and possibly other seams (e.g., *k* seams), ribbons of 2, 3, or more uniquely bonded protofilaments are created in the wall of the microtubule. This is interesting because the assembly of ribbons of three and more protofilaments has been observed in vitro (47, 48, 62, 63).

(*b*) Second, due to the unique lateral bonding of the protofilaments forming the seams, the resulting ribbons of two or three protofilaments might be expected to differ in their chemical stability; for example, because protofilaments *1* and *2* in Fig. 13 are bonded in an A lattice-like manner, or because specific MAPs are bound to these ribbons, as shown by Linck (35), the resulting ribbons might theoretically be more stable. Thus, these models offer an explanation for the resistant ribbons of two and three protofilaments observed when flagellar doublet microtubules are dissolved in sarkosyl or chaotropic ions (18, 35, 36, 39, 50, 76, 81, 82). This phenomenon of a resistant portion of the microtubule wall is not restricted to doublet microtubules, as exemplified by our consistent finding that the central-pair singlet microtubules also break down in a manner that yields stable ribbons of 4–5 protofilaments (Fig. 2 *b* and *c*). Similar micrographs have been published without comment (Figs. 1 and 3 of Meza et al. [50] are excellent examples). Furthermore, in the in vitro polymerized B tubulin singlet microtubules, the stability of such ribbons of protofilaments and associated MAPs would explain the high percentage of cold-insoluble tubulin and MAPs following solubilization of the one time tubules (see Fig. 10 *i* and Table I, Step 8). It may also be relevant that the in vitro reassembled ribbons of brain microtubule protein are cold and colchicine insoluble (62).

(*c*) Finally, seams and the stereospecifically unique sites occurring along these seams (e.g., the z sites along the j seams in Fig. 13) may specify the spatial organization of microtubule-associated components, such as dynein arms, radial spokes, and central sheath components, etc. Single classes of microtubules (i.e., flagellar B subfibers and A tubules) have been shown to be more heterogeneous than is generally recognized (33, 35, 69); thus, our models, the Figs. 13 of this and the accompanying paper, are probably oversimplified. Nevertheless, these models help one to conceptualize the mechanisms by which the macromolecular assembly of microtubules may take place. Two general principles may apply. First, the lattice of the seams may directly determine the attachment points of microtubule-associated components. For example, the 16-nm axially repeating z sites (Fig. 13) could specify the attachment of either the 16-nm repeating structures seen in negatively stained flagellar doublet microtubules (see Fig. 4) or the 16-nm periodic central-pair sheath components (40, 55). Our models show a maximum axial periodicity of only 16 nm; the 24-nm axial spacing of dynein arms and the more complex spacings of radial spokes (37) may also be specified directly but by a more chemically complex seam lattice. A second possibility, however, is that seams may specify the circumferential attachment of axoneme components but not their axial spacing. For example, dynein arms may recognize seams in the lattice but may possess their own informational molecules to determine the 24-nm axial periodicity (cf. reference 84).

In general, our hypothesis that seams direct the spatial organization of microtubule-associated components is supported by the results of Haimo et al. (22), who demonstrated that flagellar dynein binds to and crossbridges reassembled brain microtubules. In Haimo et al., 16 of the 19 reassembled brain microtubules shown in cross section possessed a single row of dynein arms. Because reassembled brain microtubules are composed predominantly of the B lattice (49), and because a pure B lattice possesses one j seam (as described in this report), we conclude that the proximal portion of flagellar dynein binds in vitro to the A lattice-like j seam and interacts distally with the B lattice portion of the adjacent, crossbridged microtubule. This concept is in agreement with our earlier analysis of dynein-microtubule interactions in the axostyle (84).

In conclusion, seams in the lattice and the existence of specialized ribbons of protofilaments are likely to be important to the native and in vitro structure and assembly of microtubules, whether they are of flagellar or nonflagellar origin.

We are grateful to Drs. David Albertini and Diane Woodrum for stimulating and invaluable discussions related to the progress of this work, and to Andrea Golden for the construction of the models (Fig. 13). R. W. Linck is indebted to Drs. Linda Amos, Aaron Klug, and Raymond Stephens, whose appreciation and perception of biological structure greatly influenced our thinking.

This work was supported by research grant GM 21527 from the U. S. National Institutes of Health to R. W. Linck, and a National Science Foundation grant PCM 78-16158 to the Department of Anatomy.

Received for publication 14 August 1980, and in revised form 12 December 1980.

NOTE ADDED IN PROOF: We have recently discovered that certain stable protofilaments of flagellar microtubules are composed principally of proteins rather similar to certain intermediate filament proteins (R. Linck, G. Langevin, G. Olson, and D. Woodrum. 1981. *Biophys. J.* 33:215*a*). We have suggested that certain intermediate filament proteins and tubulin may naturally interact to form stable protofilament ribbons, and thus longitudinal seams in flagellar and nonflagellar microtubules. Such protofilament ribbons may possess the information necessary for microtubule assembly and disassembly in vivo.

REFERENCES

1. Amos, L. A. 1979. Structure of microtubules. *In* Microtubules. K. Roberts and J. S. Hyams, editors. Academic Press Inc., New York. 1–64.
2. Amos, L. A., and A. Klug. 1974. Arrangement of subunits in flagellar microtubules. *J. Cell Sci.* 14:523–549.
3. Bell, C. W., E. Fronk, and I. R. Gibbons. 1979. Polypeptide subunits of dynein from sea urchin sperm flagella. *J. Supramol. Struct.* 11:311–317.
4. Berkowitz, S. A., J. Katagiri, H. K. Binder, and R. C. Williams, Jr. 1977. Separation and characterization of microtubule proteins from calf brain. *Biochemistry* 16:5610–5617.
5. Bibring, T., J. Baxandall, S. Denslow, and B. Walker. 1976. Heterogeneity of the alpha subunit of tubulin and the variability within a single organism. *J. Cell Biol.* 69:301–312.
6. Binder, L. I., and J. L. Rosenbaum. 1978. The in vitro assembly of flagellar outer doublet tubulin. *J. Cell Biol.* 79:500–515.
7. Brayn, J. 1974. Biochemical properties of microtubules. *Fed. Proc.* 33:152–157.
8. Caspar, D. L. D., and A. Klug. 1962. Physical principles in the construction of regular viruses. *Cold Spring Harbor Symp. Quant. Biol.* 27:1–24.
9. Cleveland, D. W., S.-Y. Hwo, and M. W. Kirschner. 1977. Purification of tau, a microtubule-associated protein that induces assembly of microtubules from purified tubulin. *J. Mol. Biol.* 116:207–225.
10. Cleveland, D. W., S.-Y. Hwo, and M. W. Kirschner. 1977. Physical and chemical properties of purified tau factor and the role of tau in microtubule assembly. *J. Mol. Biol.* 116:227–247.
11. Crepeau, R. H., B. McEwen, and S. J. Edelstein. 1978. Differences in α and β polypeptide chains of tubulin resolved by electron microscopy with image reconstruction. *Proc. Natl. Acad. Sci. U. S. A.* 75:5006–5010.
12. Dentler, W. L., S. Granett, and J. L. Rosenbaum. 1975. Ultrastructural localization of the high molecular weight proteins associated with in vitro-assembled brain microtubules. *J. Cell Biol.* 65:237–241.
13. Erickson, H. P. 1974. Microtubule surface lattice and subunit structure and observations on reassembly. *J. Cell Biol.* 60:153–167.
14. Erickson, H. P. 1978. The structure of one and two dimensional polymers of tubulin and their role in nucleation of microtubule assembly. *In* Electron Microscopy 1978. J. M. Sturgess, editor. Microscopical Society of Canada, University of Toronto, Toronto, Ontario. 3:483–494.
15. Farrel, K. W., A. Morse, and L. Wilson. 1979. Characterization of the *in vitro* reassembly of tubulin derived from stable *Strongylocentrotus purpuratus* outer doublet microtubules. *Biochemistry* 18:905–911.
16. Farrel, K. W., and L. Wilson. 1978. Microtubule reassembly *in vitro* of *Strongylocentrotus purpuratus* sperm tail outer doublet tubulin. *J. Mol. Biol.* 121:393–410.
17. Gaskin, F., C. R. Cantor, and M. L. Shelanski. 1974. Turbidimetric studies of the *in vitro* assembly and disassembly of porcine neurotubules. *J. Mol. Biol.* 89:737–758.
18. Gattass, C. R., and G. B. Witman. 1979. Protein composition of the partition protofilaments of *Chlamydomonas* flagellar outer doublet microtubules. *J. Cell Biol.* 83(2, Pt. 2):345*a* (Abstr.).

19. Gibbons, I. R. 1965. Chemical dissection of cilia. *Arch. Biol.* 76:317–352.
20. Gibbons, I. R. 1977. Structure and function of flagellar microtubules. *In* International Cell Biology 1976–1977. B. R. Brinkley and K. R. Porter, editors. The Rockefeller University Press, New York. 348–357.
21. Gibbons, I. R., and E. Fronk. 1979. A latent adenosine triphosphatase form of dynein 1 from sea urchin sperm flagella. *J. Biol. Chem.* 254:187–196.
22. Haimo, L. T., B. R. Telzer, and J. L. Rosenbaum. 1979. Dynein binds to and crossbridges cytoplasmic microtubules. *Proc. Natl. Acad. Sci. U. S. A.* 76:5759–5763.
23. Hodges, R. S., J. Sodek, L. B. Smillie, and L. Jurasek. 1973. Tropomyosin: amino acid sequence and coiled-coil structure. *Cold Spring Harbor Symp. Quant. Biol.* 37:299–310.
24. Kirschner, M. W. 1978. Microtubule assembly and nucleation. *Int. Rev. Cytol.* 54:1–71.
25. Kuriyama, R. 1976. *In vitro* polymerization of flagellar and ciliary outer fiber tubulin into microtubules. *J. Biochem. (Tokyo).* 80:153–165.
26. Laemmli, U. K. 1970. Cleavage of structural proteins during the assembly of the head of bacteriophage T4. *Nature (Lond.).* 227:680–685.
27. Langford, G. M. 1978. *In vitro* assembly of dogfish brain tubulin and the induction of coiled ribbon polymers by calcium. *Exp. Cell Res.* 111:139–151.
28. Langford, G. M. 1980. Arrangement of subunits in microtubules with 14 protofilaments. *J. Cell Biol.* 87:521–526.
29. Ledbetter, M. C., and K. R. Porter. 1964. The morphology of microtubules of plant cells. *Science (Wash, D. C.).* 144:872–874.
30. Lee, J. C., R. P. Frigon, and S. N. Timasheff. 1973. The chemical characterization of calf brain microtubule protein subunits. *J. Biol. Chem.* 248:7253–7262.
31. Lee, J. C., and S. N. Timasheff. 1977. *In vitro* reconstitution of calf brain microtubules: effects of solution variables. *Biochemistry* 16:1754–1764.
32. Lee, J. C., N. Tweedy, and S. N. Timasheff. 1978. *In vitro* reconstitution of calf brain microtubules: effects of macrotubules. *Biochemistry* 17:2783–2790.
33. Lee, V. D., K. W. Farrell, and L. Wilson. 1980. *In vitro* reassembly of flagellar A-tubule and B-subfiber tubulins. *J. Cell Biol.* 87(2, Pt. 2):252*a* (Abstr.).
34. Linck, R. W. 1973. Chemical and structural differences between cilia and flagella from the lamellibranch mollusc, *Aequipecten irradians*. *J. Cell Sci.* 12:951–981.
35. Linck, R. W. 1976. Flagellar doublet microtubules: fractionation of minor components and α-tubulin from specific regions of the A-tubule. *J. Cell Sci.* 20:405–439.
36. Linck, R. W. 1976. Fractionation of minor component proteins and tubulin from specific regions of flagellar doublet microtubules. *In* Cell Motility. R. Goldman, T. Pollard, and J. Rosenbaum, editors. Cold Spring Harbor Laboratory, Cold Spring Harbor, New York. 869–890.
37. Linck, R. W. 1979. Advances in the ultrastructural analysis of the sperm flagellar axoneme. *In* The Spermatozoan. D. W. Fawcett and J. M. Bedford, editors. Urban and Schwarzenberg, Baltimore. 99–115
38. Linck, R. W., and L. A. Amos. 1974. The hands of helical lattices in flagellar doublet microtubules. *J. Cell Sci.* 14:551–559.
39. Linck, R. W., and L. A. Amos. 1974. Flagellar doublet microtubules: selective solubilization of minor component proteins. *J. Cell Biol.* 63(2, Pt. 2):194*a* (Abstr.).
40. Linck, R. W., G. E. Olson, and G. L. Langevin. 1981. Arrangement of tubulin subunits and microtubule-associated proteins in the central pair microtubule apparatus of squid (*Loligo pealei*) sperm flagella. *J. Cell Biol.* 89:309–322.
41. Little, M. 1979. Identification of a second β-chain in pig brain tubulin. *FEBS (Fed. Eur. Biochem. Soc.) Lett.* 108:283–286.
42. Lowey, S. 1971. Myosin-molecule and filament. *In* Subunits in Biological Systems, Part A. S. N. Tamasheff and G. D. Fasman, editors. Marcel Dekker, New York. Chapter 5.
43. Lowry, O. H., N. J. Rosebrough, A. L. Farr, and R. J. Randall. 1951. Protein measurement with the Folin Phenol Reagent. *J. Biol. Chem.* 193:265–275.
44. Ludueña, R. F., E. M. Shooter, and L. Wilson. 1977. Structure of the tubulin dimer. *J. Biol. Chem.* 252:7006–7014.
45. Mandelkow, E., J. Thomas, and C. Cohen. 1977. Microtubule structure at low resolution by x-ray diffraction. *Proc. Natl. Acad. Sci. U. S. A.* 74:3370–3374.
46. Mandelkow, E.-M., and E. Mandelkow. 1979. Junctions between microtubule walls. *J. Mol. Biol.* 129:135–148.
47. Mandelkow, E.-M., E. Mandelkow, and R. Schultheiss. 1979. Correlation between structural polarity and polar assembly of brain tubulin. *J. Mol. Biol.* 135:293–299.
48. Mandelkow, E.-M., E. Mandelkow, N. Unwin, and C. Cohen. 1977. Tubulin hoops. *Nature (Lond.).* 265:655–657.
49. McEwen, B., and S. J. Edelstein. 1980. Evidence for a mixed lattice in microtubules reassembled *in vitro*. *J. Mol. Biol.* 139:123–145.
50. Meza, I., B. Huang, and J. Bryan. 1972. Chemical heterogeneity of protofilaments forming the outer doublets from sea urchin flagella. *Exp. Cell Res.* 74:535–540.
51. Murphy, D. B., and G. G. Borisy. 1975. Association of high-molecular-weight proteins with microtubules and their role in microtubule assembly *in vitro*. *Proc. Natl. Acad. Sci. U. S. A.* 72:2696–2700.
52. Murphy, D. B., K. A. Johnson, and G. G. Borisy. 1977. Role of tubulin-associated proteins in microtubule nucleation and elongation. *J. Mol. Biol.* 117:33–52.
53. Olmsted, J. B., and G. G. Borisy. 1973. Characterization of microtubule assembly in porcine brain extracts by viscometry. *Biochemistry* 12:4282–4289.
54. Olmsted, J. B., and J. M. Marcum, K. A. Johnson, C. Allen, and G. G. Borisy. 1974. Microtubule assembly: some possible regulatory mechanisms. *J. Supramol. Struct.* 2:429–450.
55. Olson, G. E., and R. W. Linck. 1977. Observations on the structural components of flagellar axonemes and central pair microtubules from rat sperm. *J. Ultrastruct. Res.* 61: 21–43.
56. Penningroth, S. M., D. W. Cleveland, and M. W. Kirschner. 1976. *In vitro* studies of the regulation of microtubule assembly. *In* Cell Motility. R. Goldman, T. Pollard, and J. Rosenbaum, editors. Cold Spring Harbor Laboratory, Cold Spring Harbor, New York. 1233–1257.
57. Pfeffer, T. A., C. F. Asnes, and L. Wilson. 1978. Polymerization and colchicine-binding properties of outer doublet microtubules solubilized by the French pressure cell. *Cytobiologie.* 16:367–372.
58. Pierson, G. B., P. R. Burton, and R. H. Himes. 1978. Alternations in number of protofilaments in microtubules assembled in vitro. *J. Cell Biol.* 76:223–228.
59. Pierson, G. B., P. R. Burton, and R. H. Himes. 1979. Wall substructure of microtubules polymerized *in vitro* from tubulin of crayfish nerve cord and fixed with tannic acid. *J. Cell Sci.* 39:89–99.
60. Pollard, T. D., and R. R. Weihing. 1974. Actin and myosin and cell movement. *CRC Crit. Rev. Biochem.* 2:1–65.
61. Sale, W. S., W.-J. Y. Tang, and I. R. Gibbons. 1979. Polypeptides associated with restoration of beat frequency in high-salt-extracted sea urchin sperm flagella. *J. Cell Biol.* 83(2, Pt. 2):177*a* (Abstr.).
62. Sandoval, I. V., and K. Weber. 1979. Polymerization of tubulin in the presence of colchicine or podophyllotoxin. Formation of a ribbon structure induced by guanylyl-5′-methylene diphosphonate. *J. Mol. Biol.* 134:159–172.
63. Sandoval, I. V., and K. Weber. 1980. Different tubulin polymers are produced by microtubule-associated proteins MPA_2 and in the presence of granosine 5′-(α,β-methylene)triphosphate. *J. Biol. Chem.* 255:8952–8954.
64. Scheele, R. B., and G. G. Borisy. 1979. *In vitro* assembly of microtubules. *In* Microtubules. K. Roberts and J. S. Hyams, editors. Academic Press Inc., New York. 175–254.
65. Shapiro, A. L., E. Viñuela, and J. V. Maizel, Jr. 1967. Molecular weight estimation of polypeptide chains by electrophoresis in SDS-polyacrylamide gels. *Biochem. Biophys. Res. Commun.* 28:815–820.
66. Sloboda, R. D., S. A. Rudolph, J. L. Rosenbaum, and P. Greengard. 1975. Cyclic AMP-dependent endogenous phosphorylation of a microtubule-associated protein. *Proc. Natl. Acad. Sci. U. S. A.* 72:177–181.
67. Stephens, R. E. 1970. Thermal fractionation of outer doublet microtubules into A- and B-subfiber components: A- and B-tubulin. *J. Mol. Biol.* 47:353–363.
68. Stephens, R. E. 1975. Structural chemistry of the axoneme: evidence for chemically and functionally unique tubulin dimers in outer fibers. *In* Molecules and Cell Movement. S. Inoue and R. E. Stephens, editors. Raven Press, New York. 181–206
69. Stephens, R. E. 1979. Equimolar heterodimers in microtubules? *J. Cell Biol.* 83(2, Pt. 2): 351*a* (Abstr.).
70. Stephens, R. E., and K. T. Edds. 1976. Microtubules: structure, chemistry and function. *Physiol. Rev.* 56:709–777.
71. Sullivan, K. F., K. W. Farrell, and L. Wilson. 1979. Developmental analysis of chick brain tubulin heterogeneity. *J. Cell Biol.* 83(2, Pt. 2):351 a (Abstr.).
72. Sund, H., K. Weber, and E. Molbert. 1967. Dissoziation der Rindlerleberkatalase in ihre Untereinheiten. *Eur. J. Biochem.* 1:400–410.
73. Tanford, C., K. Kawahara, and S. Lapanje. 1967. Proteins as random coils. I. Intrinsic viscosities and sedimentation coefficients in concentrated quanidine hydrochloride. *J. Am. Chem. Soc.* 89:729–736.
74. Tilney, L. G., J. Bryan, D. J. Bush, K. Fujiwara, M. S. Mooseker, D. B. Murphy, and D. H. Snyder. 1973. Microtubules: evidence for 13 protofilaments. *J. Cell Biol.* 59:267–275.
75. Ulman, A., M. E. Goldberg, D. Perrin, and J. Monod. 1968. On the determination of molecular weight of proteins and protein subunits in the presence of 6 M guanidine hydrochloride. *Biochemistry* 7:261–265.
76. Warner, F. D. 1974. The fine structure of the ciliary and flagellar axoneme. *In* Cilia and Flagella. M. A. Sleigh, editor. Academic Press Inc., New York. 11–37.
77. Warner, F. D., and P. Satir. 1973. The substructure of ciliary microtubules. *J. Cell Sci.* 12: 313–326.
78. Webb, B. C., and L. Wilson. 1980. Cold-stable microtubules from brain. *Biochemistry* 19: 1993–2001.
79. Weber, K., and M. Osborn. 1969. The reliability of molecular weight determinations by dodecyl sulfate-polyacrylamide gel electrophoresis. *J. Biol. Chem.* 244:4406–4412.
80. Weingarten, M. D., A. H. Lockwood, S.-Y. Hwo, and M. W. Kirschner. 1975. A protein factor essential for microtubule assembly. *Proc. Natl. Acad. Sci. U. S. A.* 72:1858–1862.
81. Witman, G. B., K. Carlson, J. Berliner, and J. L. Rosenbaum. 1972. *Chlamydomonas* flagella. I. Isolation and electrophoretic analysis of microtubules, matrix, membranes, and mastigonemes. *J. Cell Biol.* 54:507–539.
82. Witman, G. B., K. Carlson, and J. L. Rosenbaum. 1972. *Chlamydomonas* flagella. II. The distribution of tubulins 1 and 2 in the outer doublet microtubules. *J. Cell Biol.* 54:540–555.
83. Witman, G. B., D. W. Cleveland, M. D. Weingarten, and M. W. Kirschner. 1976. Tubulin requires tau for growth onto microtubule initiating sites. *Proc. Natl. Acad. Sci. U. S. A.* 73: 4070–4074.
84. Woodrum, D. T., and R. W. Linck. 1980. The structural basis of motility in the microtubular axostyle: implications for cytoplasmic microtubule structure and function. *J. Cell Biol.* 87:404–414.